MECHANISTICAL STUDIES ON THE FORMATION AND NATURE OF THE "XCN" (OCN⁻) SPECIES IN INTERSTELLAR ICES

C. J. Bennett[1,2], B. Jones[1,2], E. Knox[1], J. Perry[1], Y. S. Kim[1], and R. I. Kaiser[1,2,3]
[1] Department of Chemistry, University of Hawaii at Manoa, Honolulu, HI 96822, USA; ralfk@hawaii.edu
[2] NASA Astrobiology Institute, University of Hawaii at Manoa, Honolulu, HI 96822, USA

ABSTRACT

We conducted laboratory experiments on the interaction of ionizing radiation in the form of energetic electrons with interstellar model ices to investigate the nature and possible routes to form the "XCN" species as observed at $4.62\,\mu$m (2164 cm^{-1}) in the interstellar medium. Our laboratory experiments provided compelling evidence that the isocyanide ion (OCN⁻) presents the carrier of the "XCN" feature in interstellar ices. Most importantly, the studies exposed—based on kinetic fits of the temporal profiles of important reactants, intermediates, and products—that two formation mechanisms can lead to the production of the isocyanide ion (OCN⁻) in low-temperature interstellar ices. In carbon monoxide–ammonia ices, unimolecular decomposition of ammonia leads to reactive NH₂ and NH radical species, which in turn can react with neighboring carbon monoxide to form ultimately the isocyanide ion (OCN⁻); this process also involves a fast proton transfer to a base molecule in the surrounding ice. Second, cyanide ions (CN⁻)—formed via unimolecular decomposition of methylamine (CH₃NH₂) via a methanimine (CH₂NH) intermediate—can react with suprathermal oxygen atoms forming the isocyanide ion (OCN⁻). We also discuss that the isocyanide ion (OCN⁻) can be used as a molecular tracer to determine, for instance, the development stage of young stellar objects and also the chemical history of ices processed by ionizing radiation.

Key words: astrochemistry – comets: general – cosmic rays – infrared: ISM – ISM: molecules – methods: laboratory – molecular processes

Online-only material: color figure

1. INTRODUCTION

Three decades ago, an infrared spectroscopic study of the massive protostar W33A revealed the existence of unknown absorption bands around $4.67\,\mu$m (2141 cm^{-1}) and $4.62\,\mu$m (2164 cm^{-1}) (Soifer et al. 1979). Based on a comparison with laboratory spectra of low-temperature ices, the $4.67\,\mu$m (2141 cm^{-1}) feature was quickly determined to be solid carbon monoxide (CO); the features around $4.62\,\mu$m (2164 cm^{-1}) were proposed to be a triple-bonded nitrile and/or isonitrile (Lacy et al. 1984). Due to the tentative assignment, this feature was designated the "XCN" band. In the following years, Grim & Greenberg (1987) provided evidence that broadband ultra violet (UV) photolysis of carbon monoxide (CO) and ammonia (NH₃) ices can lead to the appearance of a band at 2165 cm^{-1}. Hudson & Moore (2000), Novozamsky et al. (2001), and Raunier et al. (2003) indicated that an acid–base reaction of ammonia with isocyanic acid (HNCO) upon warming low-temperature ices between 50 K and 90 K can also produce a band close to 2165 cm^{-1}. Therefore, the authors proposed that the OCN⁻ species might be the carrier of the $4.62\,\mu$m (2164 cm^{-1}) band. A computational study by Park & Woon (2004a) verified that an acid–base reaction might lead to the appearance of the $4.62\,\mu$m (2164 cm^{-1}) feature, suggested to likely originate from the OCN⁻ anion. Demyk et al. (1998) irradiated ices of CO:NH₃ (1:1) in the presence of electron acceptors/donors to confirm the simultaneous production of both OCN⁻ and its counter-ion, NH₄⁺, which was additionally identified at $6.85\,\mu$m (1460 cm^{-1}). However, Palumbo et al. (2000) and Bernstein et al. (2000) initially opposed the OCN⁻ designation. They argued that at least one hydrogen atom

must be part of the "XCN" species because small but distinct shifts reported in the band position of the feature at $4.62\,\mu$m (2164 cm^{-1}) were observed when deuterium was substituted for hydrogen. This shift was much smaller than the harmonic shift computationally predicted when a hydrogen atom is replaced by a deuterium atom. In a follow-up study, Hudson et al. (2001) countered that simple hydrogen bonding in the ice matrices could also account for the shift observed in the absorption spectra. The computational study of Park & Woon (2004b) confirmed this could also be a possibility. If the "XCN" band can indeed be assigned as the OCN⁻ species, the $4.62\,\mu$m (2164 cm^{-1}) feature could be utilized for determining the development stage of young stellar objects (YSOs). This survey was consecutively conducted based on observations by the *Infrared Space Observatory*, also toward protostellar disks and extragalactic starbursts.

Due to the importance of the "XCN" feature as a potential tracer of the evolutionary stage of YSOs, simulation experiments, aimed at elucidating the carrier and the inherent formation mechanism(s), were conducted in the laboratory as early as 1993. Here, ice mixtures containing water (H₂O), ammonia (NH₃), methanol (CH₃OH), methane (CH₄), nitrogen (N₂), and carbon monoxide (CO) were prepared at low temperatures between 10 K and 20 K under high vacuum conditions and exposed to either broadband UV radiation (Tegler et al. 1993; Bernstein et al. 1995; Hudson & Moore 2000; Bernstein et al. 2000; Hudson et al. 2001; Novozamsky et al. 2001) or energetic protons (Tegler et al. 1993; Hudson & Moore 2000; Palumbo et al. 2000; Hudson et al. 2001; Novozamsky et al. 2001). Only a very few investigations suggested formation mechanisms and proposed the OCN⁻ ion as the carrier. Hudson & Moore (2000) and Hudson et al. (2001) speculated that ammonia is photolyzed to form an amino radical (NH₂) plus atomic hydrogen (H). The

---

[3] Author to whom any correspondence should be addressed.

amino radical was proposed to react with carbon monoxide forming isocyanic acid (HNCO) plus atomic hydrogen, although this reaction has a significant entrance barrier. Only upon warming up, isocyanic acid likely reacted with ammonia to form OCN^- plus the ammonium ion (NH_4^+). This acid–base reaction was also proposed to dominate at elevated ice temperatures by Novozamsky et al. (2001) and Raunier et al. (2003). In all cases, bands were observed between 4.63 μm (2160 cm^{-1}) and 4.62 μm (2165 cm^{-1}).

Although mounting evidence suggests that the OCN^- anion is indeed the carrier of the "XCN" feature, the underlying reaction mechanism(s) is(are) still far from being understood. For example, crucial reaction intermediates postulated to be involved in the synthesis of OCN^- are elusive and have not been observed spectroscopically in low-temperature ices. Further, no kinetic analysis of the appearance of the OCN^- absorption was conducted; in most cases, infrared spectra were taken only at the beginning and at the end of the irradiation, but not on line and in situ during the radiation exposure as required for a detailed kinetic profile. This kinetic study is imperative to pin down the formation pathway(s). Likewise, it has not been resolved conclusively if the OCN^- feature is solely the result of an acid–base reaction upon annealing the ices, or to what extent OCN^- can be formed at 10 K without the involvement of isocyanic acid (HNCO). Based on these limiting data, we conducted systematic laboratory experiments on the interaction of energetic electrons with multiple low-temperature ice mixtures at 10 K to confirm first that the OCN^- is the carrier of the 4.62 μm (2164 cm^{-1}) feature. The main goal of our studies is to follow the formation of the molecules and of the 4.62 μm feature on line and in situ in real time during the irradiation, to extract temporal concentration profiles of the intermediates and products, and to kinetically fit these graphs so that reaction mechanism(s) can be extracted. First, we irradiated methylamine ices (CH_3NH_2) at 10 K to validate whether or not the carrier of the 4.62 μm band requires the presence of oxygen atoms as predicted for OCN^-. These experiments are compared with electron irradiation of methane–nitrogen ices studied earlier in our group (Jamieson et al. 2009). Hereafter, we increased the complexity and moved toward oxygen containing mixtures, i.e., methylamine–carbon dioxide, carbon dioxide–ammonia–hydrocarbon ices from methane (CH_4) to hexane (C_6H_{14}), as well as carbon monoxide (CO) and ammonia mixtures (NH_3). Recall that energetic electrons are formed as secondary electrons within the track of galactic cosmic ray particles upon penetrating ices in the interstellar medium (ISM) as condensed on grains and also in the outer Solar System as present, for instance, on Kuiper Belt Objects (KBOs); please refer to Bennett et al. (2009) for a detailed discussion.

2. EXPERIMENTAL DETAILS

The experiments were conducted in a contamination-free ultrahigh vacuum (UHV) chamber. A detailed description of this setup is given in Bennett et al. (2009). Briefly, the machine consists of a 15 liter cylindrical stainless steel chamber that is evacuated down to the 10^{-11} torr range by a magnetically suspended turbopump backed by an oil-free scroll pump. A rotatable, two stage closed-cycle helium refrigerator is interfaced to the lid of the machine and holds a polished silver wafer; the latter is cooled to 10.8 ± 0.2 K and serves as a substrate for the ice mixtures. The ices are condensed with the help of a precision leak valve mounted onto a linear transfer mechanism, which can be moved 5 mm in front of the target. The samples were prepared

at 10 K by depositing (1) a binary gas mixture of methylamine (CH_3NH_2; 15 torr, 99.99%; Aldrich) and carbon dioxide (CO_2; 10 torr, 99.999%; Gaspro), (2) pure methylamine (CH_3NH_2; 99.99%; Aldrich), (3) carbon dioxide (CO_2; 10 torr, 99.999%; Gaspro), ammonia (NH_3; 10 torr, 99.999%; Matheson), and a hydrocarbon mixture of methane, ethane, propane, n-butane, n-pentane, and n-hexane (CH_4, C_2H_6, C_3H_8, C_4H_{10}, C_5H_{12}, C_6H_{14}; 10 torr total hydrocarbon pressure with an equal amount of the hydrocarbons; Matheson), and (4) a binary gas mixture of carbon monoxide (CO; 677 torr, 99.99%; Specialty Gas Group) and ammonia (NH_3; 133 torr, 99.999%; Matheson). The infrared spectrum of the methylamine–carbon dioxide ice was recorded previously in our group (Holtom et al. 2005); the spectra of the pure methylamine ices exhibit—with the absence of the absorptions from carbon dioxide—identical features to those obtained from methylamine in the binary methylamine–carbon dioxide mixture (Holtom et al. 2005). The infrared spectra of the carbon dioxide–ammonia–hydrocarbon mixture depict prominent peaks as observed in pure carbon dioxide (Bennett et al. 2004), ammonia (Zheng et al. 2008), and methane ices (Bennett et al. 2006) recorded previously in our group together with the fundamentals from higher alkanes, ethane (C_2H_6), propane (C_3H_8), n-butane (C_4H_{10}), n-pentane (C_5H_{12}), and n-hexane (C_6H_{14}), as compiled in the NIST database (2009). Finally, binary ammonia–carbon monoxide spectra showed fundamentals of the carbon monoxide and ammonia obtained in earlier studies of our group (Jamieson et al. 2006; Zheng & Kaiser 2007).

Using the CASINO code (Drouin et al. 2007), which calculates the energy transfer from an electron of a defined energy to a target, each 5 keV electron loses between 2.5 and 3.1 keV of its kinetic energy while penetrating the 400–500 nm thick ice targets (Holtom et al. 2005; Bennett et al. 2006; Zheng et al. 2008); this corresponds to an averaged electronic energy transfer of about 5.2 ± 0.7 keV μm^{-1}; this number presents a similar energy loss when 10 MeV cosmic ray protons penetrate the ices, i.e., 4.8 ± 0.3 keV μm^{-1}. All ices were irradiated at 10 K with 5 keV electrons generated by an electron gun (Specs EQ-22), whereby the beam is scanned over an area of 3.0 ± 0.4 cm^2. Accounting for the extraction efficiency of 78.8% of the electrons, the target is exposed to 1.8×10^{16} electrons over an irradiation time of 60 minutes; the duration of a typical irradiation exposure. Comparing the electronic linear energy transfer in our experiments to the actual cosmic-ray energy deposition (Kaiser & Roessler 1997), 1 s of our laboratory experiments equals a processing time of interstellar ices over about $(1.9 \pm 0.3) \times 10^{11}$ s. Therefore, our laboratory experiments mimic a timescale of about 10^7 yr in the ISM; this presents a typical lifetime of an interstellar cloud. To guarantee an identification of the reaction products in the ices on line and in situ, a Fourier transform infrared spectrometer (solid state; 500–5000 cm^{-1}) was utilized (Bennett et al. 2009).

3. RESULTS

Since the main goal of our work is to investigate the formation mechanism(s), kinetics, and nature of the "XCN" band, we are reporting here only those results relevant to the "XCN" feature. Let us focus on the methylamine–carbon dioxide mixture first. With respect to "XCN," novel absorption features appeared at 2077 cm^{-1}, 2164 cm^{-1}, and 2140 cm^{-1} (Figure 1(a)). The 2077 cm^{-1} and 2164 cm^{-1} bands could be assigned to the cyanide (CN^-; ν_1) and to the isocyanide ion (OCN^-; ν_3; CN

Table 1
Compilation of New Absorption Features Observed after 1 hr of Irradiation with 5 keV Electrons
within Different Ice Mixtures Held at 10 K Relevant to the Formation of the OCN$^-$ Ion

System	Band Position (cm^{-1})	Assignment	Characterization
CH$_3$NH$_2$:CO$_2$	2077	ν_1 CN$^-$	Fundamental
	2140	ν_1 CO	Fundamental
	2164	ν_3 OCN$^-$	CN stretch
CH$_3$NH$_2$	1638	ν_4 CH$_2$NH	CN stretch
	2062	ν_1 CN$^-$	Fundamental
	4130	$2\nu_1$ CN$^-$	Overtone
NH$_3$:CO$_2$:hydrocarbons	2140	ν_1 CO	Fundamental
	2164	ν_3 OCN$^-$	CN stretch
NH$_3$:CO	2135, 2142	ν_1 CO	Fundamental
	2153	ν_3 OCN$^-$	CN stretch
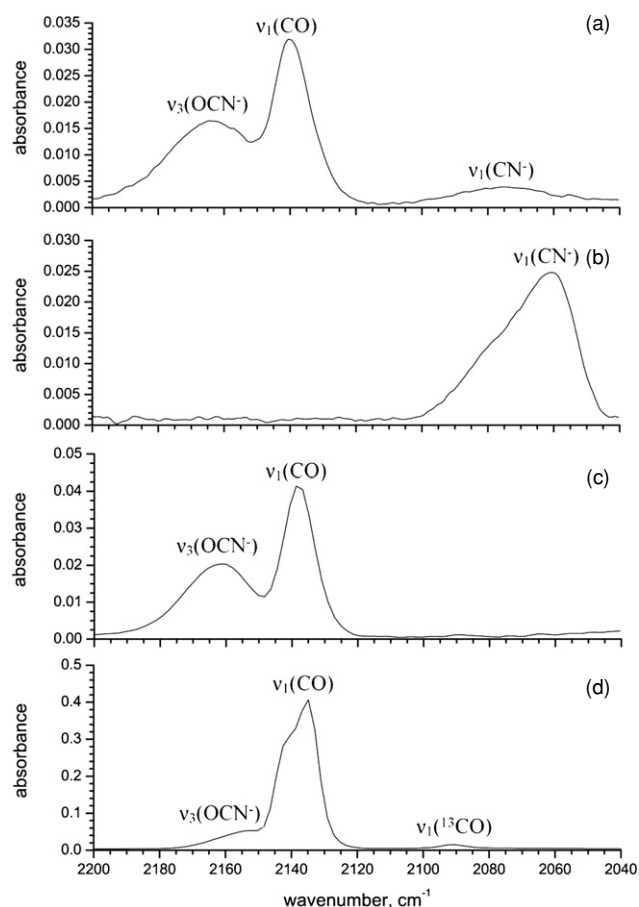
Figure 1. Infrared spectra of selected ices after irradiation over the region 2200–2040 cm^{-1} for (a) CH$_3$NH$_2$:CO$_2$, (b) CH$_3$NH$_2$, (c) NH$_3$:CO$_2$:hydrocarbons, and (d) CO:NH$_3$.

stretch), respectively (Forney et al. 1992; Hudson et al. 2001), whereas the absorption at 2140 cm^{-1} was attributed to the fundamental of carbon monoxide (CO; Jamieson et al. 2006). The band positions agree very well with previous studies, cf. Section 1, and also with those reported in the NIST database. These qualitative data present evidence that the 2164 cm^{-1} band, assigned as the OCN$^-$ species, can be produced by interaction of energetic electrons with methylamine–carbon dioxide ices at 10 K. A closer look at the temporal profiles of the absorption bands (Figure 2) indicates that carbon monoxide (CO) is formed upon the onset of the electron irradiation of the ices. Recall that carbon monoxide plus atomic oxygen are formed via the unimolecular decomposition of carbon dioxide by energetic

electrons (Bennett et al. 2004). This profile suggests that—as in the case of pure carbon dioxide ices—carbon monoxide presents a first-order reaction product. However, both the CN$^-$ and the OCN$^-$ profiles appear slightly time delayed. Here, both the cyanide and isocyanide ions can be considered as higher order reaction products.

Second, we tested the influence of carbon dioxide on the production of the "XCN" band and conducted a radiation exposure of pure methylamine ice. Here, the irradiation of pure methylamine leads to strong absorptions of methanimine (CH$_2$NH) as observed at 1638 cm^{-1} (Table 1). Additionally, the cyanide ion was observed at 2062 cm^{-1} and 4130 cm^{-1} through its fundamental and overtone, respectively (Figure 1(b)). It should be stressed that the "XCN" feature around 2164 cm^{-1} was not produced in the electron irradiation of pure methylamine ices. This result alone suggests that oxygen is very likely a component of the "XCN" band. The temporal profiles of the methanimine and cyanide ion are compiled in Figure 3.

Third, we probed if the "XCN" feature can also be produced during the electron irradiation of mixtures of ammonia, carbon dioxide, and hydrocarbon ices. As a matter of fact, the infrared spectrum of the 2200–2040 cm^{-1} region (Figure 1(c)) looks—with the exception of the missing cyanide ion—very similar to the one obtained after the electron exposure of the methylamine–carbon dioxide mixture (Figure 1(a)). Here, new novel absorption features are evident at 2164 cm^{-1} and 2140 cm^{-1} (Figure 1(c); Table 1). The 2164 cm^{-1} band belongs to the isocyanide ion (OCN$^-$; ν_3; CN stretch); the feature at 2140 cm^{-1} could be linked carbon monoxide (CO). The temporal evolution of the CO and OCN$^-$ species (Figure 4) depicts strong similarities to the irradiated methylamine–carbon dioxide ices. Carbon monoxide—as a product of the unimolecular decomposition of carbon dioxide—rises instantaneously with the start of the irradiation. On the other hand, OCN$^-$ appears to be time delayed.

Finally, we investigated to what extent the "XCN" can be formed during the electron irradiation of ammonia–carbon monoxide mixtures. The relevant range of the infrared spectrum after the irradiation is shown in Figure 1(d). Here, the absorption from OCN$^-$ at 2153 cm^{-1} is evident. We also observe carbon monoxide. However, the absorption is split into two peaks at 2135 cm^{-1} and 2142 cm^{-1}, which are attributable to carbon monoxide in two distinctive matrix environments. The corresponding decay and rise profiles of carbon monoxide and of ammonia are shown in Figure 5.

The temporal profiles shown in Figures 2–5 were produced using the following infrared bands and associated intensities (A-values) for each species: (1) CO: ν_1 at 2140 cm^{-1}, $A =$
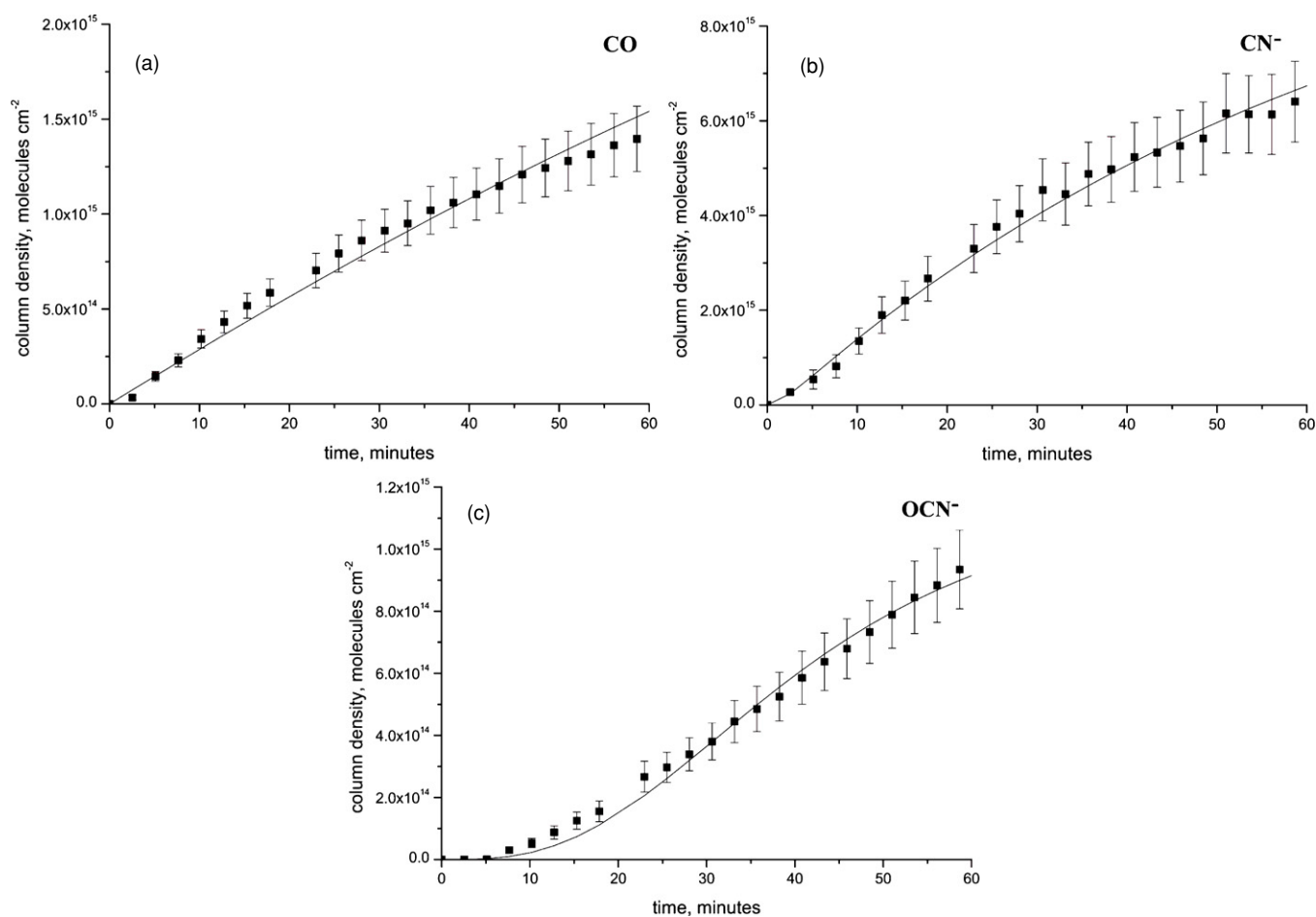
Figure 2. Temporal profiles of species produced during the electron irradiation of CH_3NH_2:CO_2 ices for (a) CO, (b) CN^-, and (c) OCN^-.
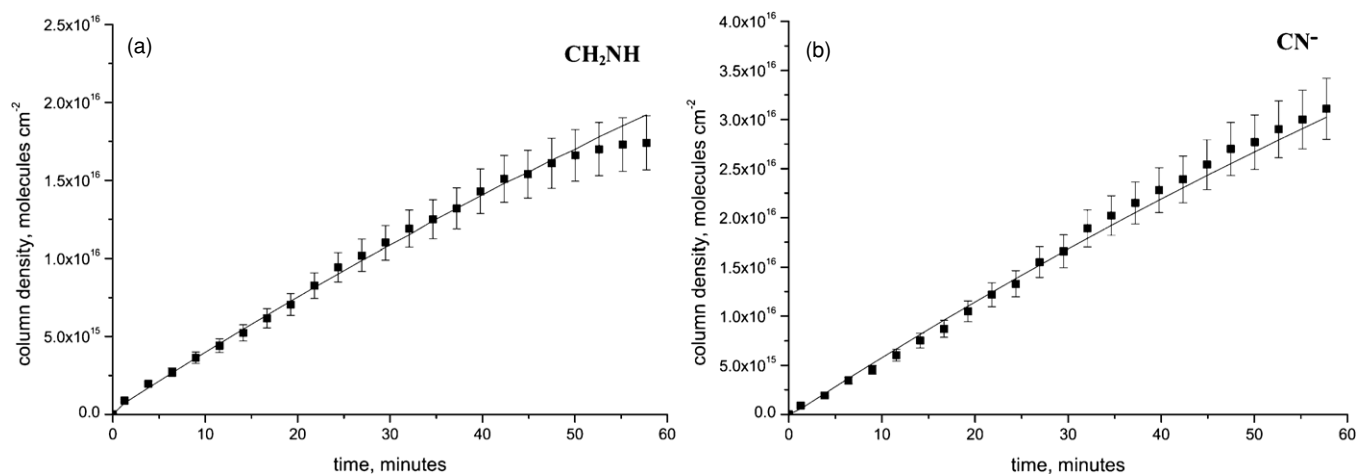

Figure 3. Temporal profiles of species produced during the electron irradiation of CH_3NH_2 ices for (a) CH_2NH and (b) CN^-.

1.1×10^{-17} cm molecule^{-1} (Jiang et al. 1975), (2) CN^-: ν_1 at ~2070 cm^{-1}, $A = 6.9 \times 10^{-18}$ cm molecule^{-1} (Georgieva & Velcheva 2006), (3) OCN^-: ν_3 at 2164 cm^{-1}, $A = 1.3 \times 10^{-16}$ cm molecule^{-1} (van Broekhuizen et al. 2004), and (4) CH_2NH: ν_4 at 1638 cm^{-1}, $A = 3.8 \times 10^{-16}$ cm molecule^{-1}, calculated at the B3LYP/6-311G(d, p) level of theory.

4. DISCUSSSION

In our experiments, we have verified experimentally that the "XCN" band can form by the interaction of energetic

electrons with methylamine–carbon dioxide, ammonia–carbon dioxide–hydrocarbon, and carbon monoxide–ammonia ices at 10 K (Table 1). Further, irradiation experiments of pure methylamine ices demonstrated explicitly that the "XCN" band cannot be produced; only absorptions of the cyanide ion (CN^-) could be detected and monitored. This indicates that oxygen presents a crucial component of the carrier of the "XCN" band. Second, the position of the "XCN" band falls around 2164 cm^{-1}; this correlates with previous assignments of the isocyanate ion (OCN^-). In ammonia-rich ices, the absorption is slightly redshifted by 11 cm^{-1} due to hydrogen bonding. Having demonstrated that
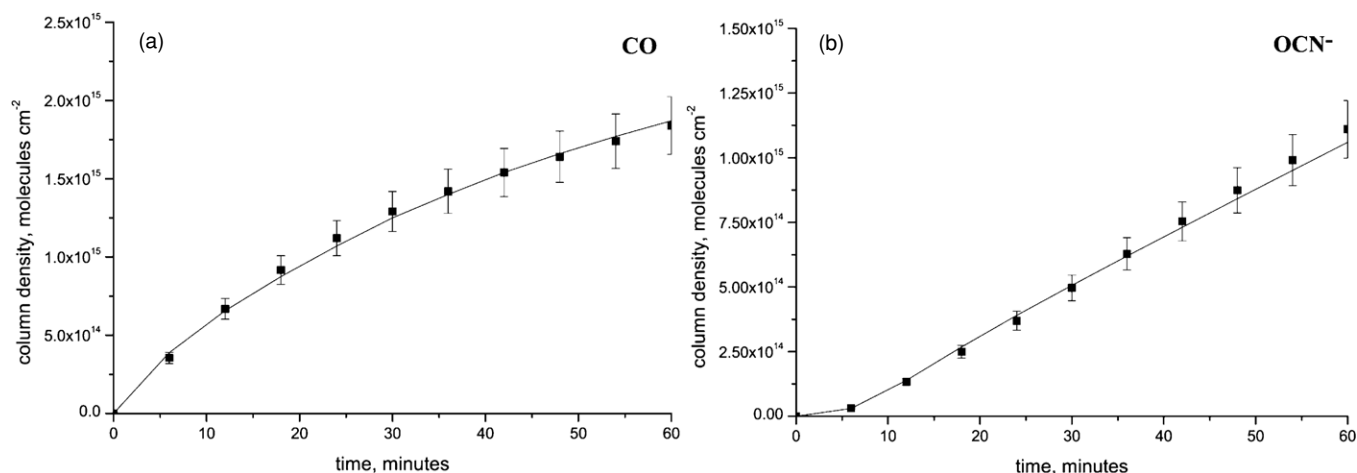
Figure 4. Temporal profiles of species produced during the electron irradiation of CO_2:NH_3:hydrocarbon ices for (a) CO and (b) OCN^-.
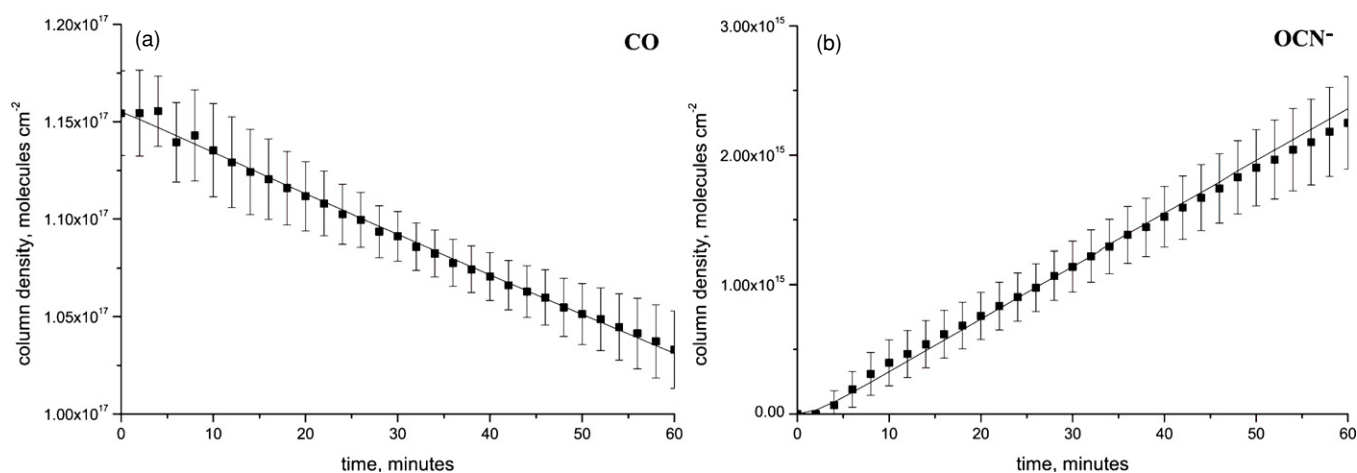

Figure 5. Temporal profiles of species produced during the electron irradiation of CO:NH_3 ices for (a) CO and (b) OCN^-.

the "XCN" band can be attributed to the oxygen-bearing isocyanate ion, we now propose possible formation mechanisms; the conclusions shown here are based on the kinetic fits of the temporal profiles as shown in Figures 2–5; the corresponding reaction mechanisms together with the rate constants are compiled in Table 2. Two reaction routes to the isocyanate ion (OCN^-) were unraveled.

4.1. Formation Via Carbon Monoxide (CO) and Nitrogen-bearing Radicals (NH/NH₂)

Identical reaction mechanisms were derived for the ammonia–carbon monoxide and carbon dioxide–ammonia–hydrocarbon ices. The reaction is initiated by an electron-induced unimolecular decomposition of the ammonia molecule as observed previously in the case of pure ammonia ices (Zheng et al. 2008) (electronic states are omitted for clarity):

$$NH_3 \rightarrow NH_2 + H \qquad (1a)$$

$$NH_3 \rightarrow NH + 2H/H_2. \qquad (1b)$$
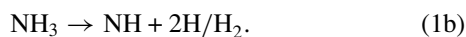
The kinetic fits alone cannot discriminate if Equation (1a) or (1b) dominates, of if both reactions contribute. For both the CO/NH_3 and CO_2/NH_3/hydrocarbon mixtures studies, the corresponding rate constants are in the same order of magnitude of $3.0–3.5 \times 10^{-6}$ s^{-1}. The kinetic fits revealed that both the NH

and NH_2 radicals can react with carbon monoxide (CO) ((2a) and (2b)):

$$CO + NH \rightarrow HNCO \qquad (2a)$$

$$CO + NH_2 \rightarrow NHCO + H. \qquad (2b)$$
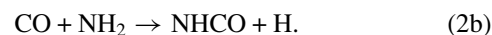
The reactions proceed formally via isocyano acid (HNCO), followed by proton transfer to form the OCN^- ion. Since we did not see any evidence in the infrared spectra of the formation of HNCO, we have to conclude that the proton transfer to a base (here: ammonia or methylamine) is fast. Kinetically, a fast proton transfer results in a bimolecular rate constant fit for the overall rate constant for reaction, which can be written as (3a) and (3b) with the base B (which could be an ammonia molecule):

$$CO + NH + B \rightarrow OCN^- + HB^+ \qquad (3a)$$

$$CO + NH_2 + B \rightarrow OCN^- + H + HB^+. \qquad (3b)$$

Note that in the CO_2/NH_3/hydrocarbon mixture, carbon monoxide is formed via unimolecular decomposition of carbon dioxide as shown also in neat carbon dioxide ices (Bennett et al. 2004). Finally, we would like to stress that thermal reactions of carbon monoxide with the NH and NH_2 radicals have likely activation energies (Zhang et al. 2004; Klippenstein & Harding 2009); however, in electron irradiated ices, these radicals are

Table 2
Summary of Rate Constants Derived from the Fitting Procedures for Each Ice System within the Current Study

System	Reaction	Rate	Rate Constant (s^{-1})
$CH_3NH_2:CO_2$[a]	$CH_3NH_2 \rightarrow CH_2NH + 2H/H_2$	k_1	3.77×10^{-4}
		$-k_1$	1.82×10^{-5}
	$CH_2NH \rightarrow HCN + 2H/H_2$	k_2	3.77×10^{-4}
	$CH_3NH_2 + HCN \rightarrow CN^- + CH_3NH_3^+$	$-k_2$	1.09×10^{-6}
	$CN^- \rightarrow X$[b]	k_3	1.14×10^{-2}
		$-k_3$	5.44×10^{-4}
	$CO_2 \rightarrow CO + O$	k_4	4.20×10^{-5}
		$-k_4$	7.08×10^{-23}[c]
	$O + CN^- \rightarrow OCN^-$	k_5	3.10×10^{-19}[c]
	$CO \rightarrow Y$[b]	k_6	3.52×10^{-5}
CH_3NH_2	$CH_3NH_2 \rightarrow CH_2NH + 2H/H_2$	k_1	3.48×10^{-5}
		$-k_1$	1.52×10^{-4}
	$CH_2NH \rightarrow HCN + 2H/H_2$	k_2	2.68×10^{-2}
	$CH_3NH_2 + HCN \rightarrow CN^- + CH_3NH_3^+$	$-k_2$	1.68×10^{-2}
	$CN^- \rightarrow X$[b]	k_3	6.19×10^{-6}
		$-k_3$	1.34×10^{-2}
$CO_2:NH_3:$hydrocarbons	$NH_3 \rightarrow NH_2 + H$	k_1	3.03×10^{-6}
	$NH_3 \rightarrow NH + 2H/H_2$		
	$CO_2 \rightarrow CO + O$	k_2	5.97×10^{-6}
	$CO \rightarrow X$[b]	k_3	3.59×10^{-4}
	$CO + NH_2 \rightarrow HOCN + H$	k_4	6.92×10^{-18}[c]
	$CO + NH \rightarrow HOCN$		
	$HOCN + NH_3 \rightarrow OCN^- + NH_4^+$		
$CO:NH_3$	$NH_3 \rightarrow NH_2 + H$	k_1	3.47×10^{-6}
	$NH_3 \rightarrow NH + 2H/H_2$		
	$CO \rightarrow X$	k_2	2.55×10^{-5}
	$CO + NH_2 \rightarrow HOCN + H$	k_3	7.06×10^{-20}[c]
	$CO + NH \rightarrow HOCN$		
	$HOCN + NH_3 \rightarrow OCN^- + NH_4^+$		

Notes.
[a] To fit the column density, a reversible reaction of carbon monoxide formation–destruction, as well as a destruction pathway for OCN^- had to be included.
[b] An additional decay pathway of CN^- and CO had to be included to fit the data.
[c] Reactions treated as bimolecular reactions ($A + B \rightarrow C$) are in units of cm^2 molecule^{-1} s^{-1}; note that the typical units for the rate of a bimolecular reaction of cm^3 molecule^{-1} s^{-1} are not applicable here, as our "concentrations" are presented in terms of column densities (molecules cm^{-2}) rather than concentration (molecules cm^{-3}).

formed with excess internal energy, which could be incorporated into the transition state of the reaction. This suprathermal (non-thermal; non-equilibrium) chemistry presents a basic requirement for both reactions. To adequately fit the carbon monoxide column density, we had to include an additional destruction pathway in both systems, schematically leading to products "X." This can be, for example, aldehydes in the hydrocarbon-bearing ices as shown for the CO/CH_4 system (Bennett et al. 2005); here, acetaldehyde (CH_3CHO) was observed at 1123 (ν_8), 1351 (ν_7), 1426 (ν_{12}), and 1728 (ν_4) cm^{-1}. To summarize, the kinetic fits depict that nitrogen-bearing radicals NH and NH_2 can react with carbon monoxide, which also involves a fast deprotonation process, to form the isocyanate ion (OCN^-) (Figure 6).

4.2. Formation Via the Cyanide Ion (CN^-) and Oxygen Atoms (O)

A detailed kinetic analysis of the kinetic profiles of the methylamine–carbon dioxide ices suggests that the isocyanate ion (OCN^-) can also be formed via reaction of the cyanide ion (CN^-) and oxygen atoms (O). During the electron decomposition, the methylamine (CH_3NH_2) molecule decomposes into methanimine (CH_2NH) (Table 2; reaction (4)):

$$CH_3NH_2 \rightarrow CH_2NH + H_2/2H. \quad (4)$$
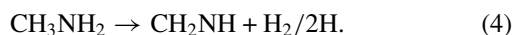
The fits suggest that further radiolysis leads de facto to the cyanide ion; this process involved the formation of HNC/HNC followed by deprotonation. In a similar manner as discussed in Section 4.1, due to the presence of multiple "base molecules" (methylamine), the deprotonation is fast, and the reaction can be globally visualized via Equation (5):

$$CH_2NH + B \rightarrow CN^- + H_2/2H + HB^+. \quad (5)$$
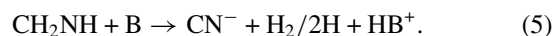
Most important, both the methanimine (CH_2NH) and cyanide ion (CN^-) species were also formed in the irradiation of pure methylamine samples. Consistent with the synthesis of OCN^- in the electron-irradiated, oxygen-bearing ices, but the formation of only CN^- in ices which do not contain oxygen (methylamine), the kinetic fits revealed that oxygen atoms can react with the cyanide ion (CN^-) to form the isocyanate ion (OCN^-) via reaction (6):

$$CN^- + O \rightarrow OCN^-. \quad (6)$$

Note that this process requires the reaction of ground and/or excited state oxygen atoms with a closed shell cyanide ion holding a $^1\Sigma_g^+$ electronic ground state. This process is similar to the reaction of ground and/or excited state oxygen atoms with carbon dioxide leading to two carbon trioxide (CO_3) isomers, i.e., the cyclic (C_{2v}) and acyclic (D_{3h}) structures (Jamieson
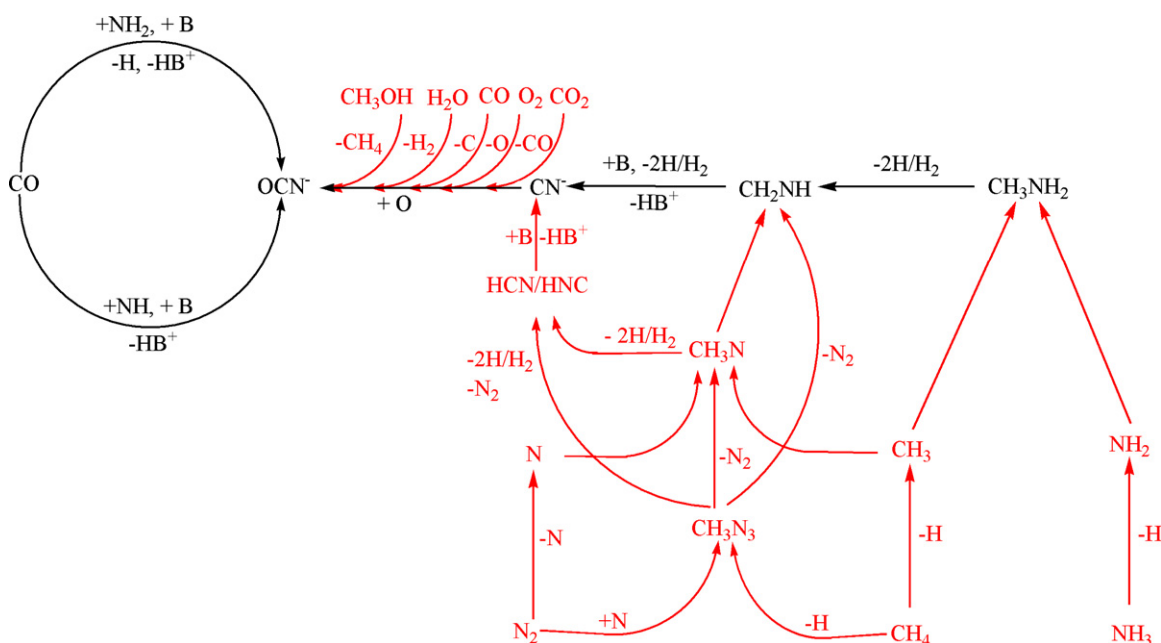
Figure 6. Summary of the observed formation pathways to the OCN$^-$ anion in interstellar analog ices; B indicates a base such as ammonia or methylamine. In red, the scheme also incorporates hydrocarbon–nitrogen chemistry in real interstellar ices as derived from previous laboratory experiments in our group. Some of the reactions involve back reactions which are omitted for clarity. Please refer to the original literature for details.

(A color version of this figure is available in the online journal.)

et al. 2006). In the case of triplet oxygen atoms (ground state), a barrier has to be overcome; this can be facilitated by suprathermal oxygen atoms released in the unimolecular decomposition of carbon dioxide.

5. ASTROPHYSICAL APPLICATIONS AND SUMMARY

To summarize, our studies verified that the isocyanide ion (OCN$^-$) presents the carrier of the "XCN" feature in interstellar ices. Most importantly, we have presented compelling evidence—based on kinetic fits of the temporal profiles of important reactants, intermediates, and products—that two formation mechanisms can lead to the production of the isocyanide ion (OCN$^-$) in low-temperature interstellar ices (Figure 6). In carbon monoxide–ammonia ices, unimolecular decomposition of ammonia leads to reactive NH$_2$ and NH radical species, which in turn can react with neighboring carbon monoxide to ultimately form the isocyanide ion (OCN$^-$); this process also involves a fast proton transfer to a base molecule in the surrounding ice. Second, cyanide ions (CN$^-$), formed via unimolecular decomposition of methylamine (CH$_3$NH$_2$) via a methanimine (CH$_2$NH) intermediate can react with suprathermal oxygen atoms forming the isocyanide ion (OCN$^-$).

Having elucidated two major routes leading to the isocyanide ion (OCN$^-$) in interstellar ices, we are placing our findings in a global, astrophysical context. Figure 6 presents an expanded incorporation of the reaction sequences leading to the isocyanide ion into an overall reaction scheme in low-temperature ices. First, although in our experiments, the oxygen atom reacting with the cyanide ion (CN$^-$) originates from carbon dioxide (CO$_2$), it should be emphasized that in realistic interstellar ices, any suprathermal oxygen atoms can lead to reaction, not only those released by carbon dioxide. Previous investigations of the

interaction of low-temperature ices with energetic electrons suggested that water (H$_2$O) can also undergo fragmentation upon radiolysis to form excited state oxygen atoms plus molecular hydrogen (H$_2$) via retro-insertion (Zheng et al. 2006). Likewise, a retro-insertion mechanism in methanol (CH$_3$OH) exposed to energetic electrons leads to electronically excited oxygen atoms and methane (CH$_4$) (Bennett et al. 2007). Moreover, molecular oxygen (O$_2$) can undergo electron-induced fragmentation producing two oxygen atoms (Bennett & Kaiser 2005). Finally, depending on the ice matrix conditions, carbon monoxide (CO) can also be fragmented to carbon and oxygen atoms (Bennett et al. 2009). Therefore, each of these atoms has the potential to react with the cyanide ion (CN$^-$) to form the isocyanide ion (OCN$^-$) if the barrier to reaction can be overcome.

Second, our experiments started from methylamine (CH$_3$NH$_2$). Previous studies suggested that in interstellar ices, methane (CH$_4$) can fragment via atomic hydrogen loss forming the methyl radical (CH$_3$) upon radiolysis (Bennett et al. 2006). Likewise, ammonia decomposes to form an amino radical (NH$_2$) plus atomic hydrogen (Zheng et al. 2008). If in close proximity, these radicals can recombine to form methylamine as well. This reaction is similar to the barrierless recombination of two hydroxyl radicals (OH) forming hydrogen peroxide (H$_2$O$_2$) (Zheng et al. 2006), of two amino radicals (NH$_2$) leading to hydrazine (NH$_2$NH$_2$) (Zheng et al. 2008), and of a hydroxyl radical (OH) with an amino radical (NH$_2$) forming hydroxylamine (NH$_2$OH) (Zheng & Kaiser 2010). Therefore, methylamine can also be formed in situ in methane–ammonia rich ices. In ices containing molecular nitrogen the situation can be more complex. Laboratory studies verified that molecular nitrogen (N$_2$) decomposes into two nitrogen atoms upon interaction with ionizing radiation (Jamieson & Kaiser 2007). A reaction of atomic nitrogen with a methyl radical can lead to the unstable CH$_3$N radical intermediate (Jamieson et al. 2009). The latter either undergoes hydrogen

migration to form methanimine (CH_2NH) or—upon unimolecular dissociation—generates hydrogen cyanide (HCN), which can react with a base via proton transfer to yield the cyanide ion (CN^-) (Jamieson et al. 2009). Alternatively, suprathermal nitrogen atoms can react with a nitrogen molecule forming the azide radical (N_3) (Jamieson & Kaiser 2007). Upon further reaction with the methyl radical, methyl azide (CH_3N_3) can be formed. The radiation chemistry of the latter is very complex (Quinto-Hernandez et al. 2010). Recent laboratory studies suggested that exposure or methylazide to ionizing radiation can form methanimine (CH_2NH), the CH_3N radical intermediate, hydrogen cyanide (HCN), and also hydrogen isocyanide (HNC). This chemistry can then be coupled with the oxygen chemistry (Figure 6(b)) to finally yield the isocyanide ion (OCN^-).

Finally, please note that carbon monoxide can have multiple sources such as the decomposition of carbon dioxide (CO_2) (Bennett et al. 2004), carbon monoxide itself, or carbon monoxide formed via recombination of carbon and oxygen atoms (Bennett et al. 2009).

In the ISM, astronomical observations of OCN^- toward low- and high-mass YSOs indicate that the abundances observed showed considerable variation from neighboring sources by factors of 10–20; typical upper limits of $\leqslant 0.85\%$ for the low-mass and $\leqslant 1.0\%$ for the higher mass YSOs were reported (van Broekhuizen et al. 2005). This is not surprising considering the fact that there are multiple formation routes to this species. Based on our laboratory studies, it is expected that the chemical composition of the ice as well as the extent of chemical processing within the local stellar environment will have strong effects on the abundance of this species. This can be coupled with the fact that there could be additional, thermal production mechanisms as the icy grains are heated as a new star forms. Here, acid–base reactions, for instance, have been found to occur rapidly upon the onset of such heating leading to increased abundances of CN^- and OCN^- (Moore & Hudson 2003; Jamieson et al. 2009). Therefore, it is expected that the band position and the abundance of the OCN^- ion can be utilized as a molecular tracer to determine, for instance, the development stage of YSOs and also the chemical history of ices processed by ionizing radiation.

REFERENCES

Bennett, C. J., Chen, S.-H., Sun, B.-J., Chang, A. H. H., & Kaiser, R. I. 2007, ApJ, 660, 1588
Bennett, C. J., Jamieson, C. S., & Kaiser, R. I. 2009, ApJS, 182, 1
Bennett, C. J., Jamieson, C. S., Mebel, A. M., & Kaiser, R. I. 2004, Phys. Chem. Chem. Phys., 6, 735
Bennett, C. J., Jamieson, C. S., Osamura, Y., & Kaiser, R. I. 2005, ApJ, 624, 1097
Bennett, C. J., Jamieson, C. S., Osamura, Y., & Kaiser, R. I. 2006, ApJ, 653, 792
Bennett, C. J., & Kaiser, R. I. 2005, ApJ, 635, 1362
Bernstein, M. P., Sandford, S. A., & Allamandola, L. J. 2000, ApJ, 542, 894
Bernstein, M. P., Sandford, S. A., Allamandola, L. J., Chang, S., & Scharberg, M. A. 1995, ApJ, 454, 327
Demyk, K., Dartois, E., d'Hendecourt, L., Jourdain de Muizon, M., Heras, A. M., & Breitfellner, M. 1998, A&A, 339, 553
Drouin, D., Couture, A. R., Joly, D., Tastet, X., Aimez, V., & Gauvin, R. 2007, Scanning, 29, 92
Forney, D. W., Thompson, W. E., & Jacox, M. E. 1992, J. Chem. Phys., 97, 1664
Georgieva, M. K., & Velcheva, E. A. 2006, Int. J. Quantum Chem., 106, 1316
Grim, R. J. A., & Greenberg, J. M. 1987, ApJ, 321, L91
Holtom, P. D., Bennett, C. J., Osamura, Y., Mason, N. J., & Kaiser, R. I. 2005, ApJ, 626, 940
Hudson, R. L., & Moore, M. H. 2000, A&A, 357, 787
Hudson, R. L., Moore, M. H., & Gerakines, P. A. 2001, ApJ, 550, 1140
Jamieson, C. S., Chang, A. H. H., & Kaiser, R. I. 2009, Adv. Space Res., 43, 1446
Jamieson, C. S., & Kaiser, R. I. 2007, Chem. Phys. Lett., 440, 98
Jamieson, C. S., Mebel, A. M., & Kaiser, R. I. 2006, ApJS, 163, 184
Jiang, G. J., Person, W. B., & Brown, K. G. 1975, J. Chem. Phys., 64, 1201
Kaiser, R. I., & Roessler, K. 1997, ApJ, 475, 144
Klippenstein, S. J., & Harding, L. B. 2009, Proc. Comb. Inst., 32, 149
Lacy, J. H., Baas, F., & Allamandola, L. J. 1984, ApJ, 276, 533
Moore, M. H., & Hudson, R. L. 2003, Icarus, 161, 486
Novozamsky, J. H., Schutte, W. A., & Keane, J. V. 2001, A&A, 379, 588
Palumbo, M. E., Pendleton, Y. J., & Strazzulla, G. 2000, ApJ, 542, 890
Park, J-Y., & Woon, D. E. 2004a, J. Phys. Chem. A, 108, 6589
Park, J-Y., & Woon, D. E. 2004b, ApJ, 601, L63
Quinto-Hernandez, A., Bennett, C. J., Kim, Y. S., Wodke, A. M., & Kaiser, R. I. 2010, ApJ, submitted
Raunier, S., Chiavassa, T., Marinelli, F., Allouche, A., & Aycard, J.-P. 2003, J. Phys. Chem. A, 107, 9335
Soifer, B. T., Puetter, R. C., Russell, R. W., Willner, S. P., Harvey, P. M., & Gillett, F. C. 1979, ApJ, 232, L53
Tegler, S. C., Weintraub, D. A., Allamandola, L. J., Sandford, S. A., Rettig, T. W., & Campins, H. 1993, ApJ, 411, 260
van Broekhuizen, F. A., Keane, J. V., & Schutte, W. A. 2004, A&A, 415, 425
van Broekhuizen, F. A., Pontoppidan, K. M., Fraser, H. J., & van Dishoeck, E. F. 2005, A&A, 441, 249
Zhang, W., Du, B., & Feng, C. 2004, J. Mol. Struct., 679, 121
Zheng, W., Jewitt, D., & Kaiser, R. I. 2006, ApJ, 639, 534
Zheng, W., Jewitt, D. C., Osamura, Y., & Kaiser, R. I. 2008, ApJ, 674, 1242
Zheng, W., & Kaiser, R. I. 2007, Chem. Phys. Lett., 440, 229
Zheng, W., & Kaiser, R. I. 2010, J. Phys. Chem. A, 114, 5251